

HeRA: an atlas of enhancer RNAs across human tissues

Zhao Zhang^{1,*†}, Wei Hong^{1,†}, Hang Ruan¹, Ying Jing¹, Shengli Li¹, Yaoming Liu¹, Jun Wang², Wenbo Li¹, Lixia Diao^{3,*} and Leng Han^{1,4,*}

¹Department of Biochemistry and Molecular Biology, McGovern Medical School at The University of Texas Health Science Center at Houston, Houston, TX 77030, USA, ²Department of Pediatrics, McGovern Medical School at The University of Texas Health Science Center at Houston, Houston, TX 77030, USA, ³Department of Bioinformatics and Computational Biology, The University of Texas MD Anderson Cancer Center, Houston, TX 77030, USA and ⁴Center for Precision Health, The University of Texas Health Science Center at Houston, Houston, TX 77030, USA

Received July 26, 2020; Revised October 06, 2020; Editorial Decision October 07, 2020; Accepted October 19, 2020

ABSTRACT

Enhancer RNA (eRNA) is a type of long non-coding RNA transcribed from DNA enhancer regions. Despite critical roles of eRNA in gene regulation, the expression landscape of eRNAs in normal human tissue remains unexplored. Using numerous samples from the Genotype-Tissue Expression project, we characterized 45 411 detectable eRNAs and identified tens of thousands of associations between eRNAs and traits, including gender, race, and age. We constructed a co-expression network to identify millions of putative eRNA regulators and target genes across different tissues. We further constructed a user-friendly data portal, Human enhancer RNA Atlas (HeRA), (<https://hanlab.uth.edu/HeRA/>). In HeRA, users can search, browse, and download the eRNA expression profile, trait-related eRNAs, and eRNA co-expression network by searching the eRNA ID, gene symbol, and genomic region in one or multiple tissues. HeRA is the first data portal to characterize eRNAs from 9577 samples across 54 human tissues and facilitates functional and mechanistic investigations of eRNAs.

INTRODUCTION

An enhancer is a type of distal DNA regulatory element that couples with a promoter to organize an enhancer–promoter loop that initiates gene expression (1). As recent studies demonstrated that an enhancer can transcribe non-coding RNA, this element has been defined as enhancer RNA (eRNA) (2). Thousands of eRNAs have been reported across different human tissues (3), and eRNA has

been shown to act as a marker for activated enhancers (4,5) and play critical roles in gene regulation (6). For example, eRNA can act as a scaffold to maintain the stability of the transcription complex (7,8). Growing evidence has suggested that eRNA expression is associated with multiple traits, characteristics, and diseases. For example, expression of the eRNA *OLMALINC* is associated with body weight by regulating the gene stearoyl-coenzyme A desaturase, which is related to serum triglyceride metabolism (9); and the expression of an eRNA is associated with autism spectrum disorders in the human brain by affecting the target gene expression (10). Biogenesis of eRNA is regulated by transcription factors (TFs), which are recruited to the DNA enhancer region to modulate chromatin accessibility and initiate eRNA transcription (6). For example, myogenic differentiation 1 (*MYOD1*) induces more than 16,000 eRNAs during myogenic differentiation (11), while estrogen receptor 1 (*ESR1*) induces thousands of eRNAs to maintain transcriptional circuitry in breast cancer (12). Furthermore, eRNA expression is critical in mediating the expression of target genes. For example, *NET1e* regulates the expression of oncogene neuroepithelial cell transforming 1 (*NET1*) in breast cancer to promote tumorigenesis (3), while *HPSEe* regulates the expression of heparanase (*HPSE*) to promote cancer invasion and metastasis (13). From these various associations with eRNAs, we sought to comprehensively investigate the expression landscape and co-expression network of eRNAs to facilitate our understanding of the mechanism of gene expression regulation and human phenotypes.

The Genotype-Tissue Expression (GTEx) project provides large numbers of RNA-seq samples and multiple traits across 54 human tissues (14). The Encyclopedia of DNA Elements (ENCODE) Project (15,16), Functional Annotation of the Mammalian Genome (FANTOM) Project (17), and

*To whom correspondence should be addressed. Tel: +1 713 500 6039; Fax: +1 713 500 0652; Email: leng.han@uth.tmc.edu

Correspondence may also be addressed to Lixia Diao. Email: ldiao@mdanderson.org

Correspondence may also be addressed to Zhao Zhang. Email: zhao.zhang@uth.tmc.edu

†The authors wish it to be known that, in their opinion, the first two authors should be regarded as Joint First Authors.

Roadmap Epigenomics Project (18) provide comprehensive annotations of enhancers. By integrating these datasets, we characterized the expression landscape and regulatory network of eRNAs and their associations with different traits across human tissues. We further developed a comprehensive data portal, the Human enhancer RNA Atlas (HeRA), to benefit the research community.

DATA COLLECTION AND PROCESSING

eRNA annotation and quantification

We collected the annotation of enhancers from ENCODE (Ensembl 87, <http://dec2016.archive.ensembl.org/index.html>) (15,16), FANTOM (<https://fantom.gsc.riken.jp/5>) (17) and the Roadmap Epigenomics Project (<http://www.roadmapepigenomics.org>) (18) (Supplementary Figure S1A). We transformed all annotations to hg19 version using Liftover (<https://genome.ucsc.edu/cgi-bin/hgLiftOver>) (19). We then integrated the eRNA annotations following the methods reported in our previous study (3). In brief, extending ± 3 kb around the middle enhancer loci, we screened enhancers that were annotated in at least two of these databases as a potential eRNA region. We excluded eRNA regions that overlapped with known transcripts (1 kb extension from both transcription start site and transcription end site), including coding genes and non-coding genes (e.g. tRNA, snoRNA and miRNAs) annotated in at least one of the following databases: Ensembl (<http://dec2016.archive.ensembl.org/index.html>) (15), UCSC (<https://genome.ucsc.edu/index.html>) (20) and GENCODE (https://www.encodegenes.org/human/release_19.html) (21) (Figure 1). We collected RNA-seq files from GTEx (phs000424.v7.p2 on 26 July 2018, Supplementary Table S1) (14). We filtered out duplicate files by retaining the one with the largest number of reads. We then followed the methods described in previous GTEx publications (22–24), and mapped these reads to the human genome (hg19) using HISAT2 (<http://daehwankimlab.github.io/hisat2/>) (25), a SNP intolerant alignment approach. We obtained 9,577 bam files across 54 human tissues from 548 donors. We then characterized eRNA expression to calculate the number of reads for eRNA using SAMtools (26) and normalized the expression value using the reads per million (RPM) method (27). We considered only eRNAs with relatively high expression levels ($\text{RPM} \geq 1$) as detectable eRNAs (Figure 1). We also used quantile normalization for all these eRNAs by R package preprocessCore (<https://github.com/bmbolstad/preprocessCore>). We further showed that co-expression analysis for trait-related eRNAs, eRNA-TF pairs and putative eRNA target genes, is highly consistent between RPM and quantile normalization in three tissues, including lung, liver, and brain cerebellum (Supplementary Figure S1B).

Trait-related eRNAs

From the GTEx portal (<https://www.gtexportal.org/home>), we collected six traits: gender, race, age, height, weight, and body mass index (BMI) (14). We calculated the association between individual eRNA expression and each trait across

tissues (28). We used the Student's *t* test to assess the statistical difference between eRNAs from male and female tissue donors and defined $|\text{fold change}| > 1.5$ and false discovery rate (FDR) < 0.05 as statistically significant. We used the analysis of variance (ANOVA) test to assess the statistical difference in eRNAs based on race and defined FDR < 0.05 as significant. Only groups with ≥ 5 samples were included in the analyses by gender and race. We used Spearman's correlation to assess the statistical difference for the continuous traits of age, weight, height, and BMI, and defined $|\text{Rho}| \geq 0.3$ and FDR < 0.05 as significant (Figure 1). All statistical analyses were analyzed by R, version 3.5.

Putative regulators of eRNAs

We collected TFs from four TF data portals, AnimalTFDB (<http://bioinfo.life.hust.edu.cn/AnimalTFDB/>) (29), DBD (<http://www.transcriptionfactor.org/>) (30), JASPAR (<http://jaspar.genereg.net/>) (31) and TF2DNA (http://www.fiserlab.org/tf2dna_db/) (32), and retained TFs that were annotated in at least one of these databases (Supplementary Figure S2A). The expression matrix of TFs in human tissues was obtained from the GTEx portal. We then identified putative regulators of eRNAs based on the co-expression between eRNA and TF across tissues. Co-expression showing Spearman's correlation $\text{Rho} \geq 0.3$ and FDR < 0.05 was considered to be significant. Furthermore, we screened potential TF binding sites (TFBS) to validate these eRNA–TF pairs. We collected TFBS based on ChIP-seq datasets from ENCODE project (<https://www.encodeproject.org/>) (33), and mapped them to those eRNAs co-expressed with TFs accordingly. Several TFs (e.g., CTCF, EP300, and RUNX3) have relatively high TFBS evidences for eRNA–TF pairs ($> 90\%$, Supplementary Figure S2B and Table S2). For those TFs with low percentage evidences, we speculated that this is due to the limited number of ChIP-seq experiments in ENCODE, that the majority of them are examined in ≤ 5 tissues/cell lines (34). We also performed GO enrichment by DAVID online tool (<https://david.ncifcrf.gov/>) (35) and observed that top 30% TFs with higher/lower TFBS discovery rates were both enriched in transcription related modules (Supplementary Figure S2C). We will update our data portal when new ChIP-seq data released by ENCODE or other consortiums.

Putative eRNA target genes

We collected gene annotations from ENSEMBL (<http://dec2016.archive.ensembl.org/index.html>) (15), GENCODE (https://www.encodegenes.org/human/release_19.html) (21) and UCSC (<https://genome.ucsc.edu/index.html>) (20) and merged them. We collected the expression matrix of these genes across human tissues from the GTEx portal. We identified putative eRNA target genes based on relatively close distance (≤ 1 MB) and significant co-expression (Spearman's correlation $\text{Rho} \geq 0.3$ and FDR < 0.05) in each tissue. We also performed random sampling (10 000 pairs) of interchromosomal pairs, and observed that the Rho is around 0.02 and FDR is around 0.3 (Supplementary Figure S3A), which is much lower than our cutoff ($\text{Rho} >$

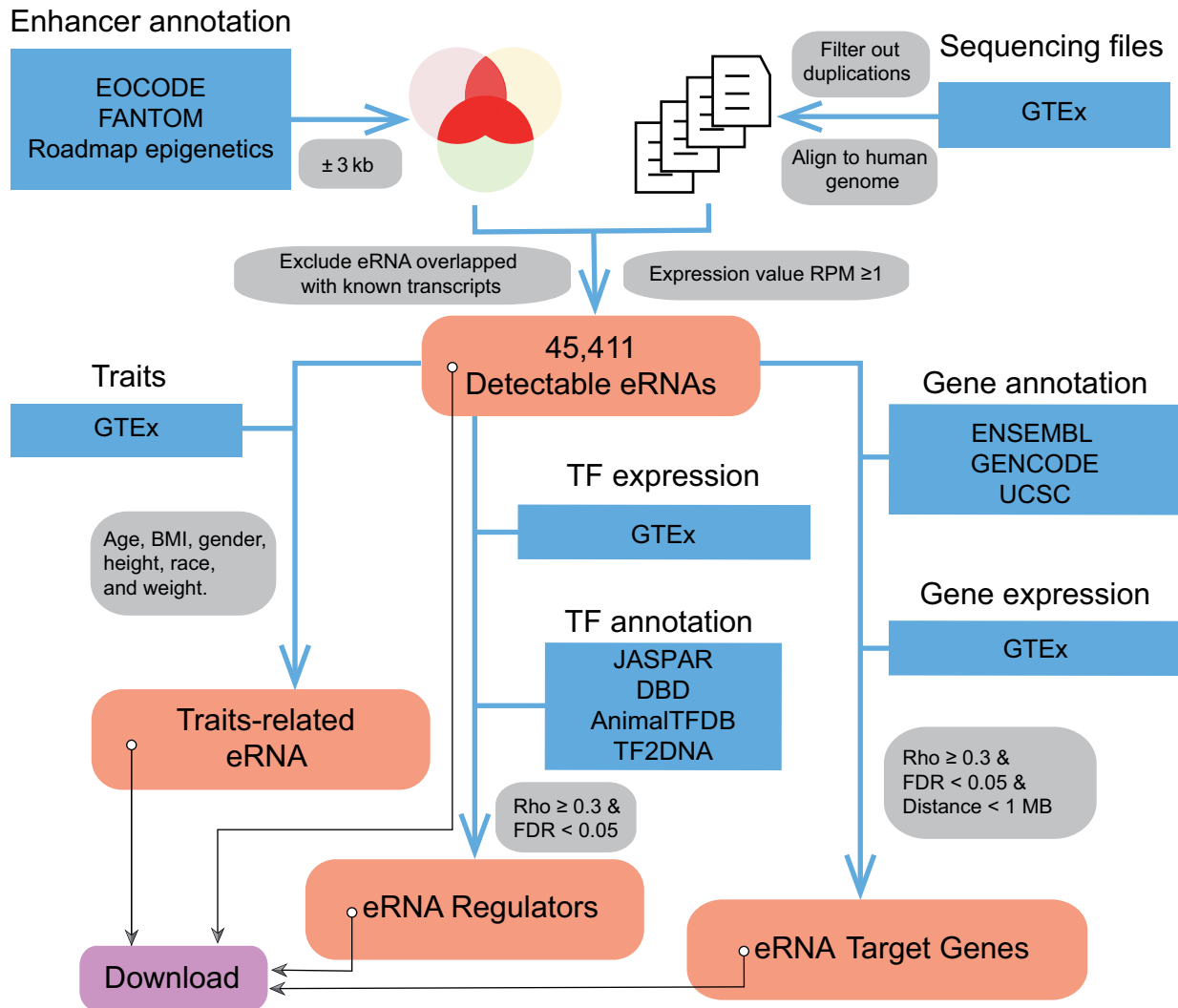


Figure 1. Computational framework for HeRA database. Blue blocks denote datasets used in this study. RNA-seq, traits and gene expression matrix were collected from GTEx. Enhancer annotation was collected from ENCODE, FANTOM and Roadmap Epigenetics Project. Transcription factors (TFs) were collected from AnimalTFDB, DBD, JASPAR and TF2DNA. Gene annotations were collected from ENSEMBL, GENCODE and UCSC. Red blocks denote processed data, including eRNA expression, traits, regulators and target genes. All processed data are available for downloading.

0.3 and $FDR < 0.05$), suggesting that our cutoff is reliable. The strength of eRNA-target gene associations is inversely dependent on the distance (Supplementary Figure S3B), which is consistent with previous studies (e.g. FANTOM5 and ENCODE) (36,37). In addition, non-strand specific RNA-seq collected in GTEx dataset is not appropriate to identify eRNA transcribed from antisense strand (<https://www.gtportal.org/home/documentationPage>) (38). Therefore, we filtered out putative associations in which the eRNA was located in the intronic region of the target gene (3,39).

Web design of HeRA

We developed the interface of HeRA using the Bootstrap 4 framework, which includes HTML, CSS and JavaScript code (<http://getbootstrap.com/>). We designed the HeRA website using Python 2.7.2, with the Django web-

framework. To perform data analyses and data plotting, we used R, version 3.5.3. We provide all the data, including eRNA expression, trait-related eRNAs, eRNA regulators, and eRNA target genes, for browsing and querying in each module of HeRA.

DATABASE CONTENT AND USAGE

Sample summary and expression landscape of human eRNAs

We collected 9577 samples across 54 normal human tissues, ranging from 5 in cervix - endocervix to 477 in muscle - skeletal, with median of 141 in liver and artery—coronary (Supplementary Table S1). In these tissues, we identified 45 411 detectable eRNAs in total. The number of detectable eRNAs in different tissues ranged from 2069 in heart—left ventricle to 14 232 in testis, with median of 4629 in esophagus—mucosa (Supplementary Table S1).

Data searching and browsing for four modules

We developed HeRA for browsing, searching, and downloading eRNA expression and trait-related eRNAs and the co-expression network. HeRA consists of four modules: *expression*, *traits*, *regulators* and *target genes* (Figure 2A). In each module, we designed two boxes: a tissue selection box, in which users can select one or more tissues for querying (Figure 2B); and an eRNA search box, in which users can search eRNAs through the genomic region, eRNA ID or gene symbol for querying (Figure 2C). For the eRNA search box, typing in a genomic region eRNA will query all eRNAs that overlap with that genomic region; typing in an eRNA ID will query the unique eRNA with this ID; and typing in a gene symbol will query all eRNAs located ± 1 MB around the transcription start site of the selected gene. In the module *traits*, we supply an additional box for trait selection, in which users can select one or more traits for querying (Figure 2D).

In the *expression* module, users can search the eRNA expression landscape across tissues. For example, ENSR00000282266, the eRNA located on chr17:6785018–6791019 within 1 MB of tumor protein P53 (*TP53*), is detectable in 32 tissues, and the mean expression value in the brain - cortex is 2.55 (Figure 2E), suggesting this might be a novel eRNA for P53. We also provided the ‘Download’ button to allow users to download sequence in FASTA format for the queried eRNAs. In the *traits* module, users can search trait-related eRNAs across tissues. For example, ENSR00000246683, the eRNA located on chrX:53211191–53217192 and within 1 MB of lysine demethylase 5C (*KDM5C*), and sourced from lung tissue, showed differential expression between male and female tissue donors (Student’s *t* test, fold-change = -1.99 and $FDR < 2.2 \times 10^{-16}$, Figure 2F). This is consistent with expression alternation of *KDM5C* between male and female in lung tissue (Supplementary Figure S4A). ENSR00000191822, the eRNA located on chr6:384543–390544 within 1 MB of interferon regulatory factor 4 (*IRF4*), and sourced from splenic tissue, showed significant association with the age of the tissue donor (Spearman correlation $Rho = 0.32$, $FDR = 0.028$, Figure 2G). This is consistent with expression correlation of *IRF4* and age in spleen tissue (Supplementary Figure S4B). In the *regulators* module, users can search putative regulators (e.g. TFs) of each eRNA across tissues. We used significant co-expression ($Rho \geq 0.3$ and $FDR < 0.05$) between eRNA and TFs to identify the putative regulatory relationship. For example, the expression of ENSR00000189515 is significantly correlated with CCCTC-binding factor (*CTCF*), a TF, in the brain – hippocampus ($Rho = 0.69$, $FDR = 1.90 \times 10^{-12}$), which suggests that *CTCF* is a potential regulator of ENSR00000189515 (Figure 2H). In the *target genes* module, users can search putative targets of eRNAs across tissues. We used close distance (within 1 MB between eRNA and gene) and significant co-expression ($Rho \geq 0.3$ and $FDR < 0.05$) to identify putative target genes. For example, ENSR00000341426 is within 1 MB of the androgen receptor (*AR*), and significantly correlates with *AR* in prostate tissue (distance = 474 778 bp, $Rho = 0.46$, $FDR = 1.39 \times 10^{-5}$), which suggests that ENSR00000341426

may regulate the expression of *AR* in the prostate (Figure 2I).

Data download and maintenance

We provide download functions for all four modules of HeRA. In the *expression* module, users can download the image file as a PDF and table file in csv format and sequence file in FASTA format for a queried eRNA in each tissue. The PDF file is consistent with the displayed image in the *expression* module (e.g. Figure 2E) and the table file includes the eRNA expression in each sample. In the *traits* module, we provide a table file for all queried results and a PDF for each queried trait (e.g. Figure 2F, G). For the *regulator* module and *target genes* module, users can download an image for each eRNA-gene pair as a PDF (e.g. Figure 2H, I). In addition, we provide a download page (<https://hanlab.uth.edu/HeRA/download>) to allow users to download the whole dataset, including expression, co-expression, and sequence for customized analysis.

SUMMARY AND FUTURE DIRECTIONS

By integrating multiple datasets, including ENCODE, FANTOM, and GTEx, we systematically quantified the expression of eRNA, trait-related eRNAs, putative eRNA regulators, and putative eRNA target genes across 54 normal human tissues. We developed a user-friendly data portal, HeRA, through which users can query, browse and download eRNA and eRNA-related events across tissues. HeRA can serve as a valuable resource for understanding the expression, association with traits, biogenesis and targets of eRNAs in human tissues. In this data resource, we followed the computational pipeline introduced by GTEx, that we used the SNP intolerant alignment. It is possible that reference mapping bias can lead to false positive co-expression patterns. Further studies are necessary to assess the impact of reference mapping bias on the co-expression studies, and whether more computationally expensive allele specific RNA-seq alignment is necessary or not. Furthermore, it is a long-known widespread consensus in the human genetic and systems biology field that for larger scale association studies, such as GWAS, eQTL and co-expression network analysis (3,40–43), RPM/RPKM/FPKM normalizations can be vulnerable to confounding artifacts. There have been a number of proposed solutions, including principal component normalization (44), that can be used to reveal sources of confounders and build co-expression network. Furthermore, it might be interesting to investigate the cross-species conservation, despite the fact that it is still challenging to characterize the cross-species conservation of ncRNAs (45), especially for the newly emerging eRNAs. We will conduct above analyses to further refine HeRA data portal in the future. In summary, we comprehensively characterized the eRNA expression landscape across human tissues and provide a useful data portal for investigating the function and underlying mechanism of eRNAs. We will continue to update this useful resource along with the booming number of related samples to benefit the research community.

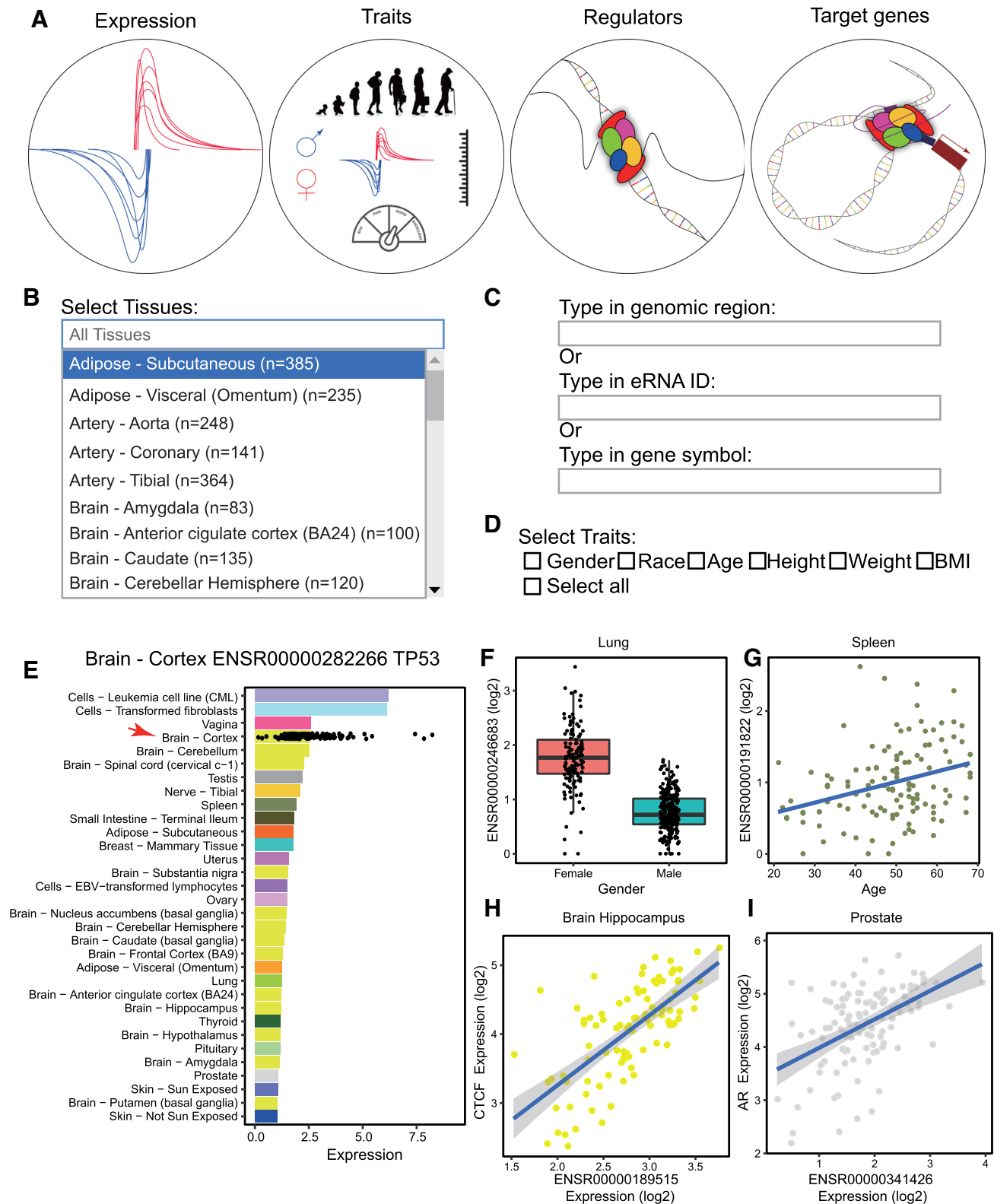


Figure 2. Overview of HeRA database. (A) Four modules of HeRA: expression, traits, regulators, and targets. (B) Interface of search boxes for tissues in each module. Users can select one or more tissues for querying. Default is all tissues. (C) Interface of search boxes for eRNA in each module. Users may query through the genomic region, eRNA ID, or gene symbol. (D) Trait selection function in the traits module. Users can select one or more traits for querying. (E) Mean expression of ENSR00000282266 across tissues (bar) and in each individual sample of brain—cortex (dot). (F) Differential expression of ENSR00000246683 in lung tissue between females and males. (G) Significant correlation of ENSR00000191822 with age in splenic tissue. (H) Co-expression of ENSR00000189515 and putative regulator *CTCF* in brain—hippocampus. (I) Co-expression of ENSR00000341426 and putative target gene *AR* in prostate tissue.

SUPPLEMENTARY DATA

Supplementary Data are available at NAR Online.

ACKNOWLEDGEMENTS

We thank LeeAnn Chastain for editorial assistance.

FUNDING

Cancer Prevention Research Institute of Texas (CPRIT) [RR150085, RP190570] to the CPRIT Scholar in Cancer Research (L.H.); Cancer Prevention Research Institute of Texas (CPRIT) [RR160083] to the CPRIT Scholar in Cancer Research (W.L.); National Institutes of Health [R56HL142704, R01HL142704, K01DE026561, R03DE025873, R01DE029014 to J.W., R21GM132778, R01GM136922 to W.L.]; UTHealth Innovation for the Cancer Prevention Research Training Program Postdoctoral Fellowship [Cancer Prevention and Research Institute of Texas grant # RP160015]. Funding for open access charge: CPRIT [RR150085].

Conflict of interest statement. None declared.

REFERENCES

1. Khoury, G. and Gruss, P. (1983) Enhancer elements. *Cell*, **33**, 313–314.
2. de Santa, F., Barozzi, I., Mietton, F., Ghisletti, S., Polletti, S., Tusi, B.K., Muller, H., Ragoussis, J., Wei, C.L. and Natoli, G. (2010) A large fraction of extragenic RNA Pol II transcription sites overlap enhancers. *PLoS Biol.*, **8**, e1000384.
3. Zhang, Z., Lee, J.H., Ruan, H., Ye, Y., Krakowiak, J., Hu, Q., Xiang, Y., Gong, J., Zhou, B., Wang, L. *et al.* (2019) Transcriptional landscape and clinical utility of enhancer RNAs for eRNA-targeted therapy in cancer. *Nat. Commun.*, **10**, 4562.
4. Hah, N., Murakami, S., Nagari, A., Danko, C.G. and Lee Kraus, W. (2013) Enhancer transcripts mark active estrogen receptor binding sites. *Genome Res.*, **23**, 1210–1223.
5. Mikhaylichenko, O., Bondarenko, V., Harnett, D., Schor, I.E., Males, M., Viales, R.R. and Furlong, E.E.M. (2018) The degree of enhancer or promoter activity is reflected by the levels and directionality of eRNA transcription. *Genes Dev.*, **32**, 42–57.
6. Li, W., Notani, D. and Rosenfeld, M.G. (2016) Enhancers as non-coding RNA transcription units: Recent insights and future perspectives. *Nat. Rev. Genet.*, **17**, 207–223.
7. Hsieh, C.L., Fei, T., Chen, Y., Li, T., Gao, Y., Wang, X., Sun, T., Sweeney, C.J., Lee, G.S.M., Chen, S. *et al.* (2014) Enhancer RNAs participate in androgen receptor-driven looping that selectively enhances gene activation. *Proc. Natl. Acad. Sci. U.S.A.*, **111**, 7319–7324.
8. Tsai, P.F., Dell'Orso, S., Rodriguez, J., Vivanco, K.O., Ko, K.D., Jiang, K., Juan, A.H., Sarshad, A.A., Vian, L., Tran, M. *et al.* (2018) A muscle-specific enhancer RNA mediates cohesin recruitment and regulates transcription in trans. *Mol. Cell*, **71**, 129–141.
9. Benhammou, J.N., Ko, A., Alvarez, M., Kaikkonen, M.U., Rankin, C., Garske, K.M., Padua, D., Bhagat, Y., Kaminska, D., Kärjä, V. *et al.* (2019) Novel lipid long intervening noncoding RNA, oligodendrocyte maturation-associated long intergenic noncoding RNA, regulates the liver steatosis gene stearoyl-coenzyme A desaturase as an enhancer RNA. *Hepatol. Commun.*, **3**, 1356–1372.
10. Yao, P., Lin, P., Gokoolparsadh, A., Assareh, A., Thang, M.W.C. and Voineagu, I. (2015) Coexpression networks identify brain region-specific enhancer RNAs in the human brain. *Nat. Neurosci.*, **18**, 1168–1174.
11. Zhao, Y., Zhou, J., He, L., Li, Y., Yuan, J., Sun, K., Chen, X., Bao, X., Esteban, M.A., Sun, H. *et al.* (2019) MyoD induced enhancer RNA interacts with hnRNPL to activate target gene transcription during myogenic differentiation. *Nat. Commun.*, **10**, 5787.
12. Li, W., Notani, D., Ma, Q., Tanasa, B., Nunez, E., Chen, A.Y., Merkurjev, D., Zhang, J., Ohgi, K., Song, X. *et al.* (2013) Functional roles of enhancer RNAs for oestrogen-dependent transcriptional activation. *Nature*, **498**, 516–520.
13. Jiao, W., Chen, Y., Song, H., Li, D., Mei, H., Yang, F., Fang, E., Wang, X., Huang, K., Zheng, L. *et al.* (2018) HPSE enhancer RNA promotes cancer progression through driving chromatin looping and regulating hnRNPU/p300/EGR1/HPSE axis. *Oncogene*, **37**, 2728–2745.
14. Lonsdale, J., Thomas, J., Salvatore, M., Phillips, R., Lo, E., Shad, S., Hasz, R., Walters, G., Garcia, F., Young, N. *et al.* (2013) The Genotype-Tissue Expression (GTEx) project. *Nat. Genet.*, **45**, 580–585.
15. Yates, A.D., Achuthan, P., Akanni, W., Allen, J., Allen, J., Alvarez-Jarreta, J., Amode, M.R., Armean, I.M., Azov, A.G., Bennett, R. *et al.* (2020) Ensembl 2020. *Nucleic Acids Res.*, **48**, D682–D688.
16. Luo, Y., Hitz, B.C., Gabdank, I., Hilton, J.A., Kagda, M.S., Lam, B., Myers, Z., Sud, P., Jou, J., Lin, K. *et al.* (2020) New developments on the Encyclopedia of DNA Elements (ENCODE) data portal. *Nucleic Acids Res.*, **48**, D882–D889.
17. Lizio, M., Abugessaisa, I., Noguchi, S., Kondo, A., Hasegawa, A., Hon, C.C., De Hoon, M., Severin, J., Oki, S., Hayashizaki, Y. *et al.* (2019) Update of the FANTOM web resource: Expansion to provide additional transcriptome atlases. *Nucleic Acids Res.*, **47**, D752–D758.
18. Chadwick, L.H. (2012) The NIH roadmap epigenomics program data resource. *Epigenomics*, **4**, 317–324.
19. Haussler, D., Zweig, A.S., Tyner, C., Speir, M.L., Rosenbloom, K.R., Raney, B.J., Lee, C.M., Lee, B.T., Hinrichs, A.S., Gonzalez, J.N. *et al.* (2019) The UCSC Genome Browser Database: 2019 update. *Nucleic Acids Res.*, **47**, D853–D858.
20. Lee, C.M., Barber, G.P., Casper, J., Clawson, H., Diekhans, M., Gonzalez, J.N., Hinrichs, A.S., Lee, B.T., Nassar, L.R., Powell, C.C. *et al.* (2020) UCSC Genome Browser enters 20th year. *Nucleic Acids Res.*, **48**, D756–D761.
21. Frankish, A., Diekhans, M., Ferreira, A.M., Johnson, R., Jungreis, I., Loveland, J., Mudge, J.M., Sisu, C., Wright, J., Armstrong, J. *et al.* (2019) GENCODE reference annotation for the human and mouse genomes. *Nucleic Acids Res.*, **47**, D766–D773.
22. Saha, A., Kim, Y., Gewirtz, A.D.H., Jo, B., Gao, C., McDowell, I.C., Engelhardt, B.E. and Battle, A. (2017) Co-expression networks reveal the tissue-specific regulation of transcription and splicing. *Genome Res.*, **27**, 1843–1858.
23. Pierson, E., Koller, D., Battle, A. and Mostafavi, S. (2015) Sharing and specificity of co-expression networks across 35 human tissues. *PLoS Comput. Biol.*, **11**, e1004220.
24. Yizhak, K., Aguet, F., Kim, J., Hess, J.M., Kübler, K., Grimsby, J., Frazer, R., Zhang, H., Haradhvala, N.J., Rosebrock, D. *et al.* (2019) RNA sequence analysis reveals macroscopic somatic clonal expansion across normal tissues. *Science*, **364**, eaaw0726.
25. Kim, D., Langmead, B. and Salzberg, S.L. (2015) HISAT: a fast spliced aligner with low memory requirements. *Nat. Methods*, **12**, 357–360.
26. Li, H., Handsaker, B., Wysoker, A., Fennell, T., Ruan, J., Homer, N., Marth, G., Abecasis, G. and Durbin, R. (2009) The Sequence Alignment/Map format and SAMtools. *Bioinformatics*, **25**, 2078–2079.
27. Mortazavi, A., Williams, B.A., McCue, K., Schaeffer, L. and Wold, B. (2008) Mapping and quantifying mammalian transcriptomes by RNA-Seq. *Nat. Methods*, **5**, 621–628.
28. Hong, W., Ruan, H., Zhang, Z., Ye, Y., Liu, Y., Li, S., Jing, Y., Zhang, H., Diao, L., Liang, H. *et al.* (2020) APAAtlas: decoding alternative polyadenylation across human tissues. *Nucleic Acids Res.*, **48**, D34–D39.
29. Hu, H., Miao, Y.R., Jia, L.H., Yu, Q.Y., Zhang, Q. and Guo, A.Y. (2019) AnimalTFDB 3.0: a comprehensive resource for annotation and prediction of animal transcription factors. *Nucleic Acids Res.*, **47**, D33–D38.
30. Kummerfeld, S.K. (2006) DBD: a transcription factor prediction database. *Nucleic Acids Res.*, **34**, D74–D81.
31. Fornes, O., Castro-Mondragon, J.A., Khan, A., Van Der Lee, R., Zhang, X., Richmond, P.A., Modi, B.P., Correard, S., Gheorghe, M., Baranašić, D. *et al.* (2020) JASPAR 2020: update of the open-access database of transcription factor binding profiles. *Nucleic Acids Res.*, **48**, D87–D92.

32. Pujato, M., Kieken, F., Skiles, A.A., Tapinos, N. and Fiser, A. (2014) Prediction of DNA binding motifs from 3D models of transcription factors; identifying TLX3 regulated genes. *Nucleic Acids Res.*, **42**, 13500–13512.
33. Moore, J.E., Purcaro, M.J., Pratt, H.E., Epstein, C.B., Shores, N., Adrian, J., Kawli, T., Davis, C.A., Dobin, A., Kaul, R. *et al.* (2020) Expanded encyclopaedias of DNA elements in the human and mouse genomes. *Nature*, **583**, 699–710.
34. Vierstra, J., Lazar, J., Sandstrom, R., Halow, J., Lee, K., Bates, D., Diegel, M., Dunn, D., Neri, F., Haugen, E. *et al.* (2020) Global reference mapping of human transcription factor footprints. *Nature*, **583**, 729–736.
35. Huang, D.W., Sherman, B.T. and Lempicki, R.A. (2009) Systematic and integrative analysis of large gene lists using DAVID bioinformatics resources. *Nat. Protoc.*, **4**, 44–57.
36. Andersson, R., Gebhard, C., Miguel-Escalada, I., Hoof, I., Bornholdt, J., Boyd, M., Chen, Y., Zhao, X., Schmidl, C., Suzuki, T. *et al.* (2014) An atlas of active enhancers across human cell types and tissues. *Nature*, **507**, 455–461.
37. Moore, J.E., Purcaro, M.J., Pratt, H.E., Epstein, C.B., Shores, N., Adrian, J., Kawli, T., Davis, C.A., Dobin, A., Kaul, R. *et al.* (2020) Expanded encyclopaedias of DNA elements in the human and mouse genomes. *Nature*, **583**, 699–710.
38. Aguet, F., Brown, A.A., Castel, S.E., Davis, J.R., He, Y., Jo, B., Mohammadi, P., Park, Y.S., Parsana, P., Segrè, A.V. *et al.* (2017) Genetic effects on gene expression across human tissues. *Nature*, **550**, 204–213.
39. Chen, H., Li, C., Peng, X., Zhou, Z., Weinstein, J.N., Caesar-Johnson, S.J., Demchok, J.A., Felau, I., Kasapi, M., Ferguson, M.L. *et al.* (2018) A pan-cancer analysis of enhancer expression in nearly 9000 patient samples. *Cell*, **173**, 386–399.
40. Gong, J., Mei, S., Liu, C., Xiang, Y., Ye, Y., Zhang, Z., Feng, J., Liu, R., Diao, L., Guo, A.Y. *et al.* (2018) PanCanQTL: systematic identification of cis-eQTLs and trans-eQTLs in 33 cancer types. *Nucleic Acids Res.*, **46**, D971–D976.
41. Joung, J., Engreitz, J.M., Konermann, S., Abudayyeh, O.O., Verdine, V.K., Aguet, F., Gootenberg, J.S., Sanjana, N.E., Wright, J.B., Fulco, C.P. *et al.* (2017) Genome-scale activation screen identifies a lncRNA locus regulating a gene neighbourhood. *Nature*, **548**, 343–346.
42. Aguet, F., Brown, A.A., Castel, S.E., Davis, J.R., He, Y., Jo, B., Mohammadi, P., Park, Y.S., Parsana, P., Segrè, A.V. *et al.* (2017) Genetic effects on gene expression across human tissues. *Nature*, **550**, 204–213.
43. Tian, D., Wang, P., Tang, B., Teng, X., Li, C., Liu, X., Zou, D., Song, S. and Zhang, Z. (2020) GWAS Atlas: a curated resource of genome-wide variant-trait associations in plants and animals. *Nucleic Acids Res.*, **48**, D927–D932.
44. Parsana, P., Ruberman, C., Jaffe, A.E., Schatz, M.C., Battle, A. and Leek, J.T. (2019) Addressing confounding artifacts in reconstruction of gene co-expression networks. *Genome Biol.*, **20**, 94.
45. Diederichs, S. (2014) The four dimensions of noncoding RNA conservation. *Trends Genet.*, **30**, 121–123.